Complete teleportation of a paraxial single-photon field

D. S. Ether,* S. P. Walborn, and N. Zagury
Instituto de Física, Universidade Federal do Rio de Janeiro, Caixa Postal 68528, Rio de Janeiro 21941-972, Rio de Janeiro, Brazil
(Received 15 November 2008; published 6 March 2009)

We discuss the *complete* teleportation of the unknown quantum state of a paraxial single-photon field. The term complete signifies that the teleportation procedure transmits the entire quantum state, which is codified in all the degrees of freedom of a paraxial single-photon field: the polarization, the transverse wave vector, and the frequency. We analyze several illustrative examples and propose a possible experimental scheme.

DOI: 10.1103/PhysRevA.79.032305 PACS number(s): 03.67.Hk, 42.50.−p, 03.67.Ac

I. INTRODUCTION

Quantum teleportation [1] is one of the most popular applications of quantum entanglement. This is due not only to the fantasy dreams of science fiction enthusiasts but also to the fact that quantum teleportation is at the core of many quantum information tasks. In principle, teleportation can be used to implement quantum logic operations for quantum computing [2–4] and to establish long-distance quantum channels using quantum repeaters [5]. Further interest stems from the fact that quantum teleportation is also an experimental reality. Photonic qubits have been successfully teleported [6–8] and even over reasonably long distances [9,10]. The continuous-variable field quadratures of a single mode of the electromagnetic field have also been transmitted via teleportation with high fidelities [11,12]. These experiments demonstrate the possibility to use teleportation to transmit quantum information between separate quantum computers, for example.

Of course the teleportation of an object consisting of even hundreds of atoms seems unrealistic. Still, one might ask, what is necessary to teleport the entire quantum state of a simple object? Here we provide an answer to this question by developing a theoretical framework for the *complete* teleportation of an unknown quantum state of a paraxial single-photon field. Here complete means that the teleportation procedure applies to all the degrees of freedom of a paraxial single-photon field, i.e., the polarization, the transverse wave vector, and the frequency.

To perform this task, a hyperentangled two-photon state [13,14]—simultaneously entangled in *all* degrees of freedom—is used as the quantum channel. Moreover, a nonlinear process realizes the destructive entangled-state measurement of all the degrees of freedom of the single photon and a member of the hyperentangled state. The nonlinear interaction is a necessary part of the protocol since it has been shown that linear operations alone cannot be used to establish more than a single ebit of entanglement [15]. In the present context, this would limit the amount of information which could be transmitted. As Lamata *et al.* [15] have shown, certain nonlinear processes plus detection may function as an entangling two-photon detector (ETPD), a device which can also be used to create a large amount of entanglement between two different systems. With an ETPD one can use quantum teleportation to send a large quantity of information, a necessary requirement if one is interested in transmitting all the degrees of freedom of a single photon. It is also interesting that the ETPD can be simulated by combining ancilla systems with linear interactions; however a large number of ancillas are necessary in principle. Recently, we have proposed an experimental scheme which implements an ETPD in the context of spatial degrees of freedom of a paraxial single-photon field [16] (see also [17] and [18] for variant proposals). Here we propose an extended scheme for all the degrees of freedom of a single-photon field.

This paper is organized as follows. In Sec. II, we discuss the complete teleportation procedure and the entangled-state measurement in the most general terms, without reference to a specific physical implementation. In Sec. III we analyze several illustrative examples and present numerical results of obtainable fidelities. In Sec. IV we discuss one possible experimental scheme which simulates the extended ETPD. Finally, in Sec. V, we conclude and briefly discuss possible extensions to other simple quantum systems.

II. COMPLETE TELEPORTATION

A. Initial state

Prior to the discussion of the protocol, let us briefly make some considerations about the state with which we are concerned. A general single-photon state can be written as

$$|\phi\rangle = \sum_s \int d\mathbf{k}u(\mathbf{k},s)|\mathbf{k},s\rangle, \tag{1}$$

where $\mathbf{k}$ and s stands for the wave vector and the polarization and the s sum corresponding to the values {0, 1} of an orthonormal polarization basis, which could be, for instance, the $\{H,V\}$ linear polarization basis. Moreover, the ket $|\mathbf{k},s\rangle$ is a Fock state which represents a single photon with well-defined wave vector and polarization. If the normalized amplitude $u(\mathbf{k},s)$ is peaked around a wave vector which defines a preferential propagation direction $\mathbf{n}_1$, we can make the paraxial approximation [19],

$$\mathbf{k} \approx \mathbf{q} + \frac{\omega}{c}\left(1 - \frac{\mathbf{q}^2c^2}{2\omega^2}\right)\mathbf{n}_1, \tag{2}$$

and rewrite the above state as

*diney@if.ufrj.br

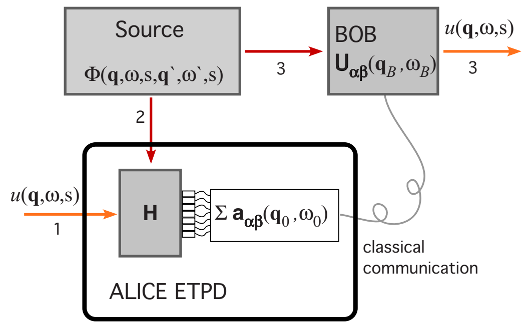

FIG. 1. (Color online) Diagram of complete teleportation procedure. The source produces a pair of hyperentangled photons 2 and 3. Alice measures photons 1 and 2 using the ETPD and communicates her measurement result to Bob, who implements the unitary operation $\mathbf{U}_{\alpha\beta}(\mathbf{q}_B,\omega_B)$.

$$|\phi\rangle_1 = \sum_s \int d\mathbf{q}\int d\omega u(\mathbf{q},\omega,s)|\mathbf{q},\omega,s\rangle_1. \tag{3}$$

Here and below, $\mathbf{q}$ is the transverse component of the wave vector $\mathbf{k}$ perpendicular to $\mathbf{n}_1$, ω is the frequency, and $|\mathbf{q},\omega,s\rangle_1 \equiv |\mathbf{q}+(\omega/c)(1-\mathbf{q}^2c^2/2\omega^2)\mathbf{n}_1,s\rangle$. Moreover, the amplitude $u(\mathbf{q},\omega,s)\equiv u(\mathbf{q}+(\omega/c)(1-\mathbf{q}^2c^2/2\omega^2)\mathbf{n}_1,s)$ is the normalized angular spectrum, and its Fourier transform $\mathcal{U}(\boldsymbol{\rho},t,s)$ at the position $\boldsymbol{\rho}$ and time t is given by

$$u(\mathbf{q},\omega,s) = \int\int d\boldsymbol{\rho}dt\mathcal{U}(\boldsymbol{\rho},t,s)e^{-i(\mathbf{q}\cdot\boldsymbol{\rho}-\omega t)}. \tag{4}$$

Figure 1 shows a diagram of the complete teleportation procedure. Suppose that Alice receives the unknown quantum state (3) and wants to transmit it to Bob using quantum teleportation [1]. In order to do so, Alice and Bob might share a hyperentangled two-photon state [13,14],

$$|\psi\rangle_{23} = \sum_s \int\int d\mathbf{q}d\mathbf{q}'\int\int d\omega d\omega'\Phi(\mathbf{q},\omega,s,\mathbf{q}',\omega',s) \times |\mathbf{q},\omega,s\rangle_2|\mathbf{q}',\omega',s\rangle_3, \tag{5}$$

where $\Phi(\mathbf{q},\omega,s,\mathbf{q}',\omega',s)$ is a normalized amplitude which we take to be

$$\Phi(\mathbf{q},\omega,s,\mathbf{q}',\omega',s) = \Lambda(s)F(\mathbf{q},\mathbf{q}')G(\omega,\omega'). \tag{6}$$

The entanglement in the transverse wave vector, frequency, and polarization depends on the form of the functions $F(\mathbf{q},\mathbf{q}')$, $G(\omega,\omega')$, and $\Lambda(s)$, respectively. Here and below, we assume $\Lambda(s)=1/\sqrt{2}$, which means that Alice and Bob shared a $|\Phi^+\rangle$ Bell state in the polarization degree of freedom. The initial three-photon state is then given by

$$|\psi_I\rangle_{123} = |\phi\rangle_1|\psi\rangle_{23}, \tag{7}$$

where photons 1 and 2 are in Alice's possession, and Bob has photon 3.

B. Joint local measurement

To implement quantum teleportation [1], Alice performs a joint local measurement on the initial state and then sends the measurement results to Bob via a classical communication channel. In the present case, this local measurement will be divided into two parts and corresponds to the action of ETPD [15].

1. Nonlinear interaction

The first part of Alice's measurement corresponds to a nonlinear interaction between fields 1 and 2, which in general can be described by the effective Hamiltonian

$$\mathbf{H} = \sum_{i=1}^{2} \mathbf{H}_i, \tag{8}$$

where

$$\mathbf{H}_1 \equiv g_1\sum_{s=0}^{1}\int\int d\mathbf{q}d\mathbf{q}'\int\int d\omega d\omega'\mathbf{a}_1(\mathbf{q},\omega,s)\mathbf{a}_2(\mathbf{q}',\omega',s) \times \mathbf{a}_4^\dagger(\mathbf{q}+\mathbf{q}',\omega+\omega',s^\perp) + \text{H.c.}, \tag{9}$$

$$\mathbf{H}_2 \equiv g_2\sum_{s=0}^{1}\int\int d\mathbf{q}d\mathbf{q}'\int\int d\omega d\omega'\mathbf{a}_1(\mathbf{q},\omega,s)\mathbf{a}_2(\mathbf{q}',\omega',s^\perp) \times \mathbf{a}_5^\dagger(\mathbf{q}+\mathbf{q}',\omega+\omega',s) + \text{H.c.} \tag{10}$$

In these expressions, $\mathbf{a}_i^\dagger(\mathbf{q},\omega,s)$ and $\mathbf{a}_i(\mathbf{q},\omega,s)$ are creation and annihilation operators of photons with wave vector $\mathbf{k}=\mathbf{q}+(\omega/c)(1-\mathbf{q}^2c^2/2\omega^2)\mathbf{n}_i$ and polarization s. These Hamiltonians describe nonlinear physical processes in which two photons are destroyed and another one is created: the Hamiltonian $\mathbf{H}_1$ destroys photons with the same polarization s and creates another one with an orthogonal polarization $s^\perp$. Moreover, the Hamiltonian $\mathbf{H}_2$ destroys photons with orthogonal polarizations s and $s^\perp$ and creates another one with the polarization s. Assuming that the coupling constants g_1 and g_2 are small, the time evolution of initial state (7) may be well approximated by

$$|\psi\rangle = e^{-i\mathbf{H}t/\hbar}|\psi_I\rangle_{123}|\text{vac}\rangle_{45} \approx (\mathbf{1}-i\mathbf{H}t/\hbar)|\psi_I\rangle_{123}|\text{vac}\rangle_{45}. \tag{11}$$

Considering only the first perturbation correction, which can be identified by the presence of a photon in direction 4 or 5, we then have

$$|\psi^{(1)}\rangle = N\mathbf{H}|\psi_I\rangle_{123}|\text{vac}\rangle_{45}, \tag{12}$$

where N is a normalization constant.

2. Acquisition of information

The second part of Alice's measurement is the acquisition of information about the wave vector and the polarization of the created photon. In order to acquire this information, Alice uses photoelectric detection, filters, and polarizers, which implement the action of one of the following annihilation operators $\mathbf{a}_{\alpha\beta}(\mathbf{q}_0,\omega_0)$ on state (12),

$$\mathbf{a}_{00}(\mathbf{q}_0,\omega_0) = \mathbf{a}_4(\mathbf{q}_0,\omega_0,0_X),$$

$$\mathbf{a}_{01}(\mathbf{q}_0,\omega_0) = \mathbf{a}_5(\mathbf{q}_0,\omega_0,0_X),$$

$$\mathbf{a}_{10}(\mathbf{q}_0,\omega_0) = \mathbf{a}_4(\mathbf{q}_0,\omega_0,1_X),$$

$$\mathbf{a}_{11}(\mathbf{q}_0,\omega_0) = \mathbf{a}_5(\mathbf{q}_0,\omega_0,1_X). \tag{13}$$

Each operator $\mathbf{a}_{\alpha\beta}(\mathbf{q}_0,\omega_0)$ destroys a photon with wave vector $\mathbf{k}_0=\mathbf{q}_0+(\omega_0/c)(1-\mathbf{q}_0^2c^2/2\omega_0^2)\mathbf{n}_j$, where $j=4$ or 5, and a polarization 0_X or 1_X, where 0_X (1_X) stands for the elements of a linear polarization basis whose directions make 45° (135°) with the 0 (1) elements of the standard basis. In the Appendix, Sec. 1, it is shown that the application of one of these operators selects only one of the terms of state (12), and the state after the measurement will be

$$|\psi_{\alpha\beta}\rangle \propto \mathbf{a}_{\alpha\beta}(\mathbf{q}_0,\omega_0)|\psi^{(1)}\rangle. \tag{14}$$

Alice then sends her measurement results to Bob, who is in possession of photon 3.

C. Unitary operation and final state

After receiving Alice's measurement results, Bob performs on his field the unitary operation $\mathbf{U}_{\alpha\beta}(\mathbf{q}_B,\omega_B)$ defined as

$$\mathbf{U}_{\alpha\beta}(\mathbf{q}_B,\omega_B)|\mathbf{q},\omega,s\rangle = \boldsymbol{\sigma}_Z^{\alpha}\boldsymbol{\sigma}_X^{\beta}|\mathbf{q}+\mathbf{q}_B,\omega+\omega_B,s\rangle, \tag{15}$$

where $\boldsymbol{\sigma}_Z^{\alpha}\boldsymbol{\sigma}_X^{\beta}$ corresponds to $\mathbf{1}$ or the Pauli matrices $\boldsymbol{\sigma}_Z$, $\boldsymbol{\sigma}_X$, and $\boldsymbol{\sigma}_Z\boldsymbol{\sigma}_X$ depending on the values 0 and 1 of the labels α and β. This operation corresponds to shifts $\mathbf{q}_B$ and ω_B in the tranverse wave vector and frequency, along with a polarization rotation $\boldsymbol{\sigma}_Z^{\alpha}\boldsymbol{\sigma}_X^{\beta}$. Generally, $\mathbf{q}_B$ and ω_B depend on $\mathbf{q}_0$ and ω_0 along as well as the central wave vector $\mathbf{q}_p$ and central frequency ω_p of the amplitude $\Phi(\mathbf{q},\omega,s,\mathbf{q}',\omega',s)$ of the hyperentangled two-photon state. As a result, applying Eq. (15) into Eq. (14), the final state of the system is given by

$$|\psi_F^{\alpha\beta}\rangle \propto \mathbf{U}_{\alpha\beta}(\mathbf{q}_B,\omega_B)|\psi_{\alpha\beta}\rangle. \tag{16}$$

To illustrate the above results, let us first consider the limiting case in which Alice and Bob shared a maximally hyperentangled two-photon state, i.e., an EPR type state [20] in the $\mathbf{q}$ and ω degrees of freedom together with a Bell state in polarization. In this case, the functions $F(\mathbf{q},\mathbf{q}')$ and $G(\omega,\omega')$ in amplitude (6) take the following forms:

$$F(\mathbf{q},\mathbf{q}') \propto \delta^2(\mathbf{q}+\mathbf{q}'-\mathbf{q}_p),$$

$$G(\omega,\omega') \propto \delta(\omega+\omega'-\omega_p). \tag{17}$$

In the Appendix, Sec. 1 it is shown that, for example, in the case where $\alpha=\beta=1$, we have

$$|\psi_F^{11}\rangle \propto \sum_s \int d\mathbf{q}\int d\omega u(\Delta\mathbf{q}-\mathbf{q}_B,\Delta\omega-\omega_B,s)|\mathbf{q},\omega,s\rangle_3, \tag{18}$$

where $\Delta\mathbf{q}\equiv\mathbf{q}+\mathbf{q}_0-\mathbf{q}_p$ and $\Delta\omega\equiv\omega+\omega_0-\omega_p$, and we have excluded the state of the other fields, which are all in the vacuum. Using shifts $\mathbf{q}_B=\mathbf{q}_0-\mathbf{q}_p$ and $\omega_B=\omega_0-\omega_p$, Bob has

$$|\psi_F^{11}\rangle \propto |\phi\rangle_3, \tag{19}$$

which corresponds to the perfect teleportation of field 1.

Rather than directly obtaining the final state in this limiting case, suppose that we substitute Eq. (17) in state (14). Again, for $\alpha=\beta=1$, we find

$$|\psi_{11}\rangle \propto \sum_s (-1)^s\int d\mathbf{q}\int d\omega u(\Delta\mathbf{q},\Delta\omega,s)|\mathbf{q},\omega,s^{\perp}\rangle_3. \tag{20}$$

Using Eq. (4), we can rewrite this expression as

$$|\psi_{11}\rangle \propto \sum_s (-1)^s\int\int d\mathbf{q}d\omega\int\int d\boldsymbol{\rho}dt\mathcal{U}(\boldsymbol{\rho},t,s) \times e^{-i[(\Delta\mathbf{q})\cdot\boldsymbol{\rho}-\Delta\omega t]}|\mathbf{q},\omega,s^{\perp}\rangle_3. \tag{21}$$

Applying the operation,

$$\mathcal{U}(\boldsymbol{\rho},t,s) \to e^{i(\mathbf{q}_B\cdot\boldsymbol{\rho}-\omega_B t)}\mathcal{U}(\boldsymbol{\rho},t,s), \tag{22}$$

where again $\mathbf{q}_B=\mathbf{q}_0-\mathbf{q}_p$ and $\omega_B=\omega_0-\omega_p$ together with the polarization rotation $|\mathbf{q},\omega,s^{\perp}\rangle_3\to\boldsymbol{\sigma}_Z\boldsymbol{\sigma}_X|\mathbf{q},\omega,s^{\perp}\rangle_3=(-1)^s|\mathbf{q},\omega,s\rangle_3$, we find $|\psi\rangle\to|\psi_F^{11}\rangle\propto|\phi\rangle_3$. Therefore, Bob's tranverse wave vector and frequency correction shifts can also be viewed as an operation which includes in the amplitude $\mathcal{U}(\boldsymbol{\rho},t,s)$ a phase dependent term in position and time, respectively.

The figure of merit of the teleportation procedure success is quantified by the fidelity, which for two pure states $|u\rangle$ and $|v\rangle$ is defined as $\mathcal{F}=|\langle u|v\rangle|^2$ [21]. In our case, these two states are the final state of photon 3 and the initial state of photon 1. However, since final state (16) is conditioned on Alice's measurement results, i.e., which operator (13) has been realized, the fidelity depends on these results,

$$\mathcal{F}_{\alpha\beta}(\mathbf{q}_0,\omega_0) = |\langle\phi|\psi_F^{\alpha\beta}\rangle_3|^2. \tag{23}$$

Thus, we also define the average fidelity over these measurement results,

$$\bar{\mathcal{F}} = \sum_{\alpha,\beta}\int d\mathbf{q}_0\int d\omega_0 p_{\alpha\beta}(\mathbf{q}_0,\omega_0)\mathcal{F}_{\alpha\beta}(\mathbf{q}_0,\omega_0), \tag{24}$$

where $p_{\alpha\beta}(\mathbf{q}_0,\omega_0)$ is a weight function given by

$$p_{\alpha\beta}(\mathbf{q}_0,\omega_0) = \mathrm{Tr}[\boldsymbol{\varrho}_{45}\Pi_{\alpha\beta}(\mathbf{q}_0,\omega_0)], \tag{25}$$

such that $\boldsymbol{\varrho}_{45}=\mathrm{Tr}_{123}(|\psi^{(1)}\rangle\langle\psi^{(1)}|)$, with $|\psi^1\rangle$ being given by Eq. (12), is the system density operator before the annihilation of the created photon and $\Pi_{\alpha\beta}(\mathbf{q}_0,\omega_0)=\mathbf{a}_{\alpha\beta}^{\dagger}(q_0,\omega_0)|\mathrm{vac}\rangle\langle\mathrm{vac}|\mathbf{a}_{\alpha\beta}(q_0,\omega_0)$ is a one-photon Fock state projector. This weight function corresponds to the probability of measuring the created photon with wave vector $\mathbf{k}_0=\mathbf{q}_0+(\omega_0/c)(1-\mathbf{q}_0^2c^2/2\omega_0^2)\mathbf{n}_j$, where $j=4$ or 5 and polarization 0_X or 1_X.

III. EXAMPLES

Since an EPR type state corresponds to a limiting case, let us analyze some more realistic examples. Let us assume that the functions in Eq. (6) are given by

$$F(\mathbf{q},\mathbf{q}') = v(\mathbf{q}+\mathbf{q}')\gamma(\mathbf{q}-\mathbf{q}'),$$

$$G(\omega,\omega') = t(\omega+\omega')\mu(\omega-\omega'), \tag{26}$$

which are typical in experiments using photons from spontaneous parametric down-conversion (SPDC) with pulsed pump lasers. Moreover, let us suppose that the state of photon 1 is given by

$$u(\mathbf{q},\omega,s) = f(\mathbf{q})g(\omega)\lambda(s), \tag{27}$$

which is also a function with all the degrees of freedom uncorrelated and corresponds to a field in the *quasi-cw* pulsed wave approximation [19].

Using these expressions in Eq. (16), together with the shifts $\mathbf{q}_B=\mathbf{q}_0-\mathbf{q}_p$ and $\omega_B=\omega_0-\omega_p$, and substituting the result in Eq. (23), we find

$$\mathcal{F}_{\alpha\beta}(\mathbf{q}_0,\omega_0) = \mathcal{M}(\mathbf{q}_0)\mathcal{T}(\omega_0), \tag{28}$$

where

$$\mathcal{M}(\mathbf{q}_0) = \left| C\int\int d\mathbf{q}d\mathbf{q}' f^*(\mathbf{q}')f(\mathbf{q})v(\mathbf{q}'-\mathbf{q}+\mathbf{q}_p) \times \gamma(2\mathbf{q}_0-\mathbf{q}'-\mathbf{q}-\mathbf{q}_p)\right|^2,$$

$$\mathcal{T}(\omega_0) = \left| D\int\int d\omega d\omega' g^*(\omega')g(\omega)t(\omega'-\omega+\omega_p) \times \mu(2\omega_0-\omega'-\omega-\omega_p)\right|^2, \tag{29}$$

with C and D being normalization constants. Note that Eq. (28) does not depend on the indices α and β since the polarization channel, given by Eq. (6), corresponds to a Bell state. Furthermore, the average fidelity $\overline{\mathcal{F}}$ [Eq. (24)] is also given by

$$\overline{\mathcal{F}} = \overline{\mathcal{M}}\overline{\mathcal{T}}, \tag{30}$$

where

$$\overline{\mathcal{M}} = \int d\mathbf{q}_0 \mathcal{M}(\mathbf{q}_0),$$

$$\overline{\mathcal{T}} = \int d\omega_0 \mathcal{T}(\omega_0). \tag{31}$$

Let us consider that $v(\mathbf{q})$, $\gamma(\mathbf{q})$, $t(\omega)$, and $\mu(\omega)$ are given by Gaussian functions,

$$v(\mathbf{q}) = J(q_X-q_{pX},0,\sigma_{q+})J(q_Y-q_{pY},0,\sigma_{q+}),$$

$$\gamma(\mathbf{q}) = J(q_X,0,\sigma_{q-})J(q_Y,0,\sigma_{q-}),$$

$$t(\omega) = J(\omega-\omega_p,0,\sigma_{\omega+}),$$

$$\mu(\omega) = J(\omega,0,\sigma_{\omega-}), \tag{32}$$

where $\mathbf{q}_p$ and ω_p are the central transverse wave vector and central frequency of the entangled pair, and

$$J(a,b,\Delta) = \frac{\sqrt{2}}{\Delta\sqrt{\pi}}\exp\left(-\frac{a^2}{2\Delta^2}-iab\right). \tag{33}$$

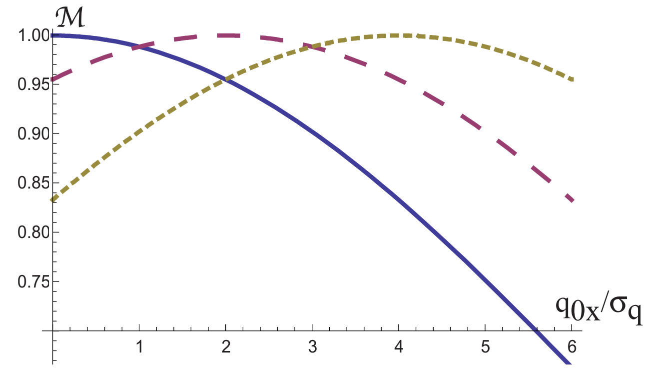

FIG. 2. (Color online) Transverse wave vector fidelity $\mathcal{M}$ dependence on the ratio q_{0X}/σ_q for the values $q_{cX}/\sigma_q=0,2,4$ (solid, large dashed, and small dashed lines, respectively) and parameters $q_{pX}/\sigma_q=0$, $\sigma_{q+}/\sigma_q=1/2$, and $\sigma_{q-}/\sigma_q=5$. The maximum fidelity is obtained when $q_{0X}=q_{cX}$.

A. Transverse wave vector and frequency displaced Gaussian field

As our first example, suppose that amplitude (27) of photon 1 is described by

$$f(\mathbf{q}) = J(q_X-q_{cX},0,\sigma_q)J(q_Y-q_{cY},0,\sigma_q),$$

$$g(\omega) = J(\omega-\omega_c,0,\sigma_\omega), \tag{34}$$

which correspond to Gaussian functions displaced in the transverse wave vector and frequency spaces by the central values $\mathbf{q}_c$ and ω_c, respectively.

Figure 2 shows the dependence of the tranverse wave vector fidelity $\mathcal{M}$ on the ratio q_{0X}/σ_q between the detected transverse wave-vector X component and the amplitude width of photon 1 for different central values $q_{cX}/\sigma_q=0,2,4$ and for the parameters $q_{pX}=0$, $\sigma_{q+}/\sigma_q=1/2$, and $\sigma_{q-}/\sigma_q=5$. For these chosen parameters, we see that fidelities achieve maximum values when the detected transverse wave vector has precisely the central value $\mathbf{q}_c$.

Another important result is given by Fig. 3, which shows the dependence of the average tranverse wave vector fidelity $\overline{\mathcal{M}}$ given by Eq. (24) on the parameters σ_{q+}/σ_q and σ_{q-}/σ_q, which quantifies the quality of the quantum channel. Plots are shown for $q_{cx}/\sigma_q=1$, $q_{px}=0$. Moreover, the average is calculated on a detector area of size $Q/\sigma_q=4.2$. We see that high average fidelities are achieved when the ratios σ_{q+}/σ_q and σ_{q-}/σ_q become small and large, respectively. This corresponds to a more entangled pair, the limit $\sigma_{q+}/\sigma_q\to 0$ and $\sigma_{q-}/\sigma_q\to\infty$ corresponding to an EPR state [20].

The numerical results for the frequency are similar to the above results since the tranverse wave vector and frequency fidelities given by Eq. (29) are nearly equal. Nevertheless, in Fig. 4 we show the frequency fidelity $\mathcal{T}$ dependence with the ratio ω_0/σ_ω of the detected frequency ω_0 per amplitude width σ_ω of photon 1 for $\omega_c/\sigma_\omega=2.5\times10^4$ and $\omega_p/\sigma_\omega=5.0\times10^4$, which correspond to picosecond pulses with central frequencies $\omega_c\approx 2.5\times10^{15}$ Hz and $\omega_p\approx 5.0\times10^{15}$ Hz, respectively, and spectral widths $\sigma_\omega\approx 100$ GHz. Moreover,

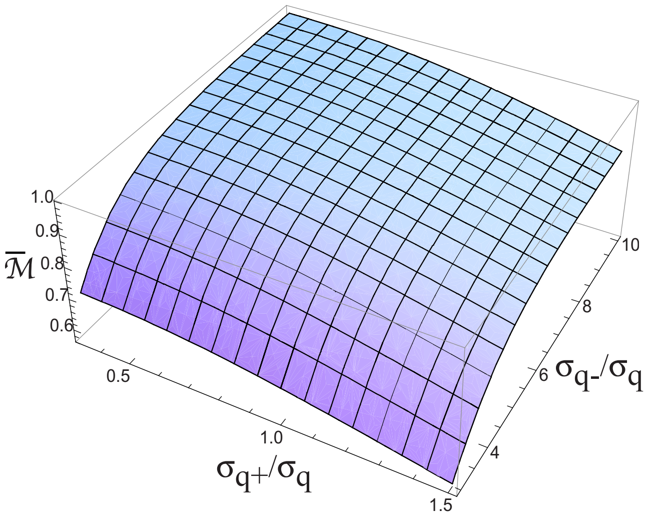

FIG. 3. (Color online) Average tranverse wave vector fidelity $\overline{\mathcal{M}}$ as a function of σ_{q+}/σ_q and σ_{q-}/σ_q for $q_{cX}/\sigma_q=1$, $q_{pX}/\sigma_q=0$, and a square detection area of side $Q/\sigma_q=4.2$. Higher average fidelities are achieved when $\sigma_{q+}/\sigma_q \to 0$ and $\sigma_{q-}/\sigma_q \to \infty$.

$\sigma_{\omega+}/\sigma_\omega=1/2$ and $\sigma_{\omega-}/\sigma_\omega=20$. We see that high fidelities are achieved when the detected frequency ω_0 matches the entangled pair central frequency ω_p.

B. Position and time displaced Gaussian field

Next we consider the case in which amplitude of photon 1 is given by

$$f(\mathbf{q}) = J(q_X,x_c,\sigma_q)J(q_Y,y_c,\sigma_q),$$

$$g(\omega) = J(\omega-\omega_c,t_c,\sigma_\omega). \tag{35}$$

These functions describe a Gaussian amplitude which is displaced in position space by $\mathbf{r}_c=(x_c,y_c)$ and also in frequency and time by ω_c and t_c, respectively. In Fig. 5, we analyze the averaged tranverse wave vector fidelity $\overline{\mathcal{M}}$ dependence with the product $x_c\sigma_q$ for the fixed parameters $q_{pX}/\sigma_q=q_{cX}/\sigma_q=0$, $\sigma_{q+}/\sigma_q=1/2$, $\sigma_{q-}/\sigma_q=10$, and $Q/\sigma_q=4.2$. We see that

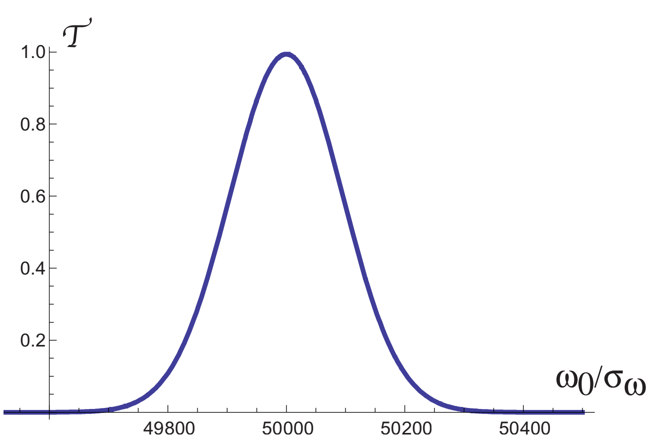

FIG. 4. (Color online) Frequency fidelity $\mathcal{T}$ as a function of ω_0/σ_ω, for $\omega_c/\sigma_\omega=2.5\times10^4$, $\omega_p/\sigma_\omega=5.0\times10^4$, $\sigma_{\omega+}/\sigma_\omega=1/2$, and $\sigma_{\omega-}/\sigma_\omega=20$. The maximum fidelity is achieved for $\omega_0=\omega_p$.

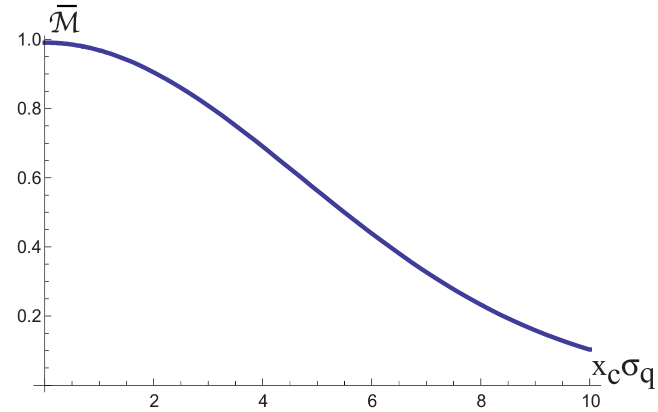

FIG. 5. (Color online) Averaged tranverse wave vector fidelity $\overline{\mathcal{M}}$ as a function of $x_c\sigma_q$, for $q_{pX}/\sigma_q=q_{cX}/\sigma_q=0$, $\sigma_{q+}/\sigma_q=1/2$, $\sigma_{q-}/\sigma_q=10$, and $Q/\sigma_q=4.2$. The average fidelity decreases as the displacement x_c becomes large.

the more the amplitude of photon 1 is spatially displaced, the less the average fidelity is. This fidelity deterioration is understandable since larger displacements correspond to a small overlap between the amplitude of photons 1 and 2. As a result, information about the amplitude of photon 1 is lost.

The two examples described above indicate that, given that the teleportation scheme works for distributions shifted in Fourier conjugate variables (i.e., transverse position and transverse wave vector and also time and frequency), it should be possible to transmit any single-photon field with a reasonable fidelity.

IV. PROPOSALS FOR AN EXPERIMENTAL REALIZATION

The complete teleportation procedure requires three main steps: (i) preparation of a hyperentangled two-photon state, (ii) implementation of the complete ETPD, and (iii) implementation of Bob's unitary operation. In this section, we discuss a possible experimental realization of these three steps.

A. Preparation of hyperentangled states

Hyperentangled two-photon states have been created with SPDC [13,14]. The wave vector and frequency entanglement stem from the momentum and energy conservation and are inherent in the SPDC process. Polarization entanglement is generated using either the "crossed cone" [22] or two-crystal source [23]. As a result, one of these geometries can produce a hyperentangled two-photon state accurately described by state (5).

B. Implementation of an ETPD

The realization of an efficient ETPD presents more of an experimental challenge. As pointed out in [15], an entangling measurement of continuous degrees of freedom can be realized by some nonlinear interaction which couples fields 1 and 2 with fields 4 and 5. For instance, in the sum frequency generation (SFG) nonlinear process [24], the fields involved are constrained by the conservation of energy and momentum, $\omega_1+\omega_2=\omega_{\mathrm{SFG}}$ and $\hbar(\mathbf{k}_1+\mathbf{k}_2)=\hbar\mathbf{k}_{\mathrm{SFG}}$. Under appropriate

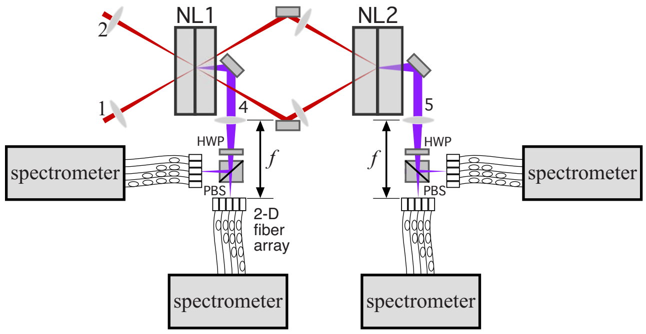

FIG. 6. (Color online) A possible implementation of Alice's ETPD on photons 1 and 2. NL represents one of the nonlinear processes discussed in the text. The HWP, set at 22,5°, together with the PBS allows the complete Bell-state polarization analysis. The Fourier transform lens system and two-dimensional (2D) optical fiber bundle perform the wave-vector measurement. The fibers are time multiplexed to a spectrometer, which performs the frequency measurement. The detection time determines through which fiber the photon passed. The final information is given by $\mathbf{q}_0$, ω_0, and the indices α and β.

experimental conditions [25], the resulting Hamiltonian describing this process is approximated by [26–29]

$$\mathbf{H} = A\int\int d\mathbf{q}d\mathbf{q}'\int\int d\omega d\omega' \mathbf{a}_1(\mathbf{q},\omega)\mathbf{a}_2(\mathbf{q}',\omega') \times \mathbf{a}^{\dagger}_{\mathrm{SFG}}(\mathbf{q}+\mathbf{q}',\omega+\omega') + \mathrm{H.c.}, \tag{36}$$

where the factor A is responsible for the conversion efficiency and depends on the susceptibility tensor and dimensions of the crystal, as well as the frequency and polarization of the fields. This Hamiltonian has the same wave vector and frequency structure of Hamiltonians (9) and (10). As a result, a single SFG crystal is capable of implementing the frequency and wave-vector parts of the ETPD. To create the polarization dependence and thus completely realize Hamiltonians (9) and (10), one can arrange pairs of crystals of different types (I or II), as described in [8] (see the Appendix, Sec. 2 for additional information).

Figure 6 illustrates an experimental scheme of an ETPD. NL1 and NL2 are nonlinear SFG interactions, which are realized by two type-I and -II crystals with perpendicular optical axes. After these interactions, the generated fields 4 and 5 are sent through a Fourier lens system, a half-wave plate (HWP), a polarizing beam splitter (PBS), and a two-dimensional array of optical fibers. The lens systems map the transverse wave vector at the output of the crystals to the transverse position at the plane containing the fibers. Thus, the wave-vector measurement is performed by determining through which fiber the photon passes. The HWP, which is aligned at 22,5°, together with the PBS allows for the separation of the 0_X and 1_X polarization components and thus permits the complete Bell-state polarization measurement [8]. Each fiber leads to a spectrometer for frequency measurement. The fibers are of significantly different length, so that the detection time of the photon corresponds to which fiber it passed through and thus also to the result of the wave-vector measurement. To measure the frequency of a single photon, the spectrometer will require an array of detectors or optical fibers. When a single detector finally clicks at time τ, it contains information about all degrees of freedom. Alice then sends the information about her measurement results ($\mathbf{q}_0$, ω_0, α, and β) to Bob.

SFG of single photons in bulk crystals has been demonstrated experimentally in Ref. [8]; however the efficiency is typically very low. We expect that a more promising alternative is to use a stimulated four-wave mixing (FWM) process of the type $\omega_{p1}+\omega_{p2}\rightarrow\omega_s+\omega_i$, in which mode s is seeded with an intense laser field. As shown recently by Ou [30], this "two-photon annihilator" can be constructed to have near unity efficiency, provided the seed laser is sufficiently intense.

C. Bob's unitary operation

After receiving information from Alice, Bob must perform a unitary operation $\mathbf{U}_{\alpha\beta}(\mathbf{q}_B,\omega_B)$, which is composed of three parts: a polarization rotation, a transverse wave vector and frequency shifts. The polarization rotation can be implemented trivially by a pair of wave plates or Pockells cells. As explained in Sec. II, the tranverse wave vector correction shift can also be viewed as an inclusion of a phase dependent term $\exp(i\mathbf{q}_B\cdot\boldsymbol{\rho})$ in the field profile, which can be easily implemented by a spatial light modulator. Finally, the frequency shift can be realized by performing another SFG of photon 3 with an intense laser beam of frequency ω_B so that $\omega_3+\omega_B\rightarrow\omega_1$. High efficiencies of 93% have been recently achieved in this process [31].

V. CONCLUSION

We propose a general scheme for the complete teleportation of the unknown quantum state of a paraxial single-photon field. The term complete means that information encoded in all photon's degrees of freedom, i.e., polarization, transverse wave vector, and frequency, are teleported. To perform this task, a hyperentangled two-photon state together with a nonlinear device is required. We have examined several illustrative examples, which show that high fidelities are achieved, and discussed a possible experimental scheme. Moreover, our general scheme is also valid for mixture states of a single-photon field. We also remark that the idea of a complete teleportation should be applicable to more complex systems, such as atoms or Bose-Einstein condensates [32]. For instance, nonlinear interactions between Bose-Einstein condensates have already been realized [33], together with theoretical proposal of entanglement creation between Bose-Einstein condensates [34]. Combining these two resources together with an appropriate unitary operation, it might be possible to realize the complete teleportation of a Bose-Einstein condensate.

Recently, we became aware of a similar scheme which has been proposed recently [35].

ACKNOWLEDGMENTS

The authors would like to thank the Brazilian funding agencies CNPq, FAPERJ, CAPES, and the Millennium Institute for Quantum Information for financial support, and E. Solano and R. L. de Matos Filho for helpful discussions.

APPENDIX

In this Appendix we have shown some calculations which have been omitted in the text but may help the reader.

1. Complete teleportation

First of all, let us rewrite in Eq. (12) in a more detailed way,

$$|\psi^{(1)}\rangle = N\sum_{i=1}^{2} \mathbf{H}_i|\psi_I\rangle_{123}|\text{vac}\rangle_{45} \equiv |\zeta\rangle + |\eta\rangle, \tag{A1}$$

where we define

$$|\zeta\rangle \equiv N\mathbf{H}_1|\psi_I\rangle_{123}|\text{vac}\rangle_{45},$$

$$|\eta\rangle \equiv N\mathbf{H}_2|\psi_I\rangle_{123}|\text{vac}\rangle_{45}. \tag{A2}$$

Using Eqs. (3), (5), (9), and (10), we find

$$|\zeta\rangle = Ng_1\sum_s \int\int\int d\mathbf{q}d\mathbf{q}'d\mathbf{q}''\int\int\int d\omega d\omega' d\omega'' \times u(\mathbf{q},\omega,s)\Phi(\mathbf{q}',\omega',s,\mathbf{q}'',\omega'',s)|\mathbf{q}'',\omega'',s\rangle_3 \times|\mathbf{q}+\mathbf{q}',\omega+\omega',s^{\perp}\rangle_4,$$

$$|\eta\rangle = Ng_2\sum_s \int\int\int d\mathbf{q}d\mathbf{q}'d\mathbf{q}''\int\int\int d\omega d\omega' d\omega'' \times u(\mathbf{q},\omega,s)\Phi(\mathbf{q}',\omega',s^{\perp},\mathbf{q}'',\omega'',s^{\perp})|\mathbf{q}'',\omega'',s^{\perp}\rangle_3 \times|\mathbf{q}+\mathbf{q}',\omega+\omega',s\rangle_5, \tag{A3}$$

where, for simplicity, we have excluded the other fields, which are all in the vacuum state. Next we perform the polarization change of basis in photons 4 and 5 subspaces,

$$|\mathbf{q},\omega,0\rangle = \frac{1}{\sqrt{2}}(|\mathbf{q},\omega,0_X\rangle + |\mathbf{q},\omega,1_X\rangle),$$

$$|\mathbf{q},\omega,1\rangle = \frac{1}{\sqrt{2}}(|\mathbf{q},\omega,0_X\rangle - |\mathbf{q},\omega,1_X\rangle), \tag{A4}$$

which allow us to rewrite the above states as

$$|\zeta\rangle = \frac{Ng_1}{\sqrt{2}}\sum_s \int\int\int d\mathbf{q}d\mathbf{q}'d\mathbf{q}''\int\int\int d\omega d\omega' d\omega'' \times u(\mathbf{q},\omega,s)\Phi(\mathbf{q}',\omega',s,\mathbf{q}'',\omega'',s)|\mathbf{q}'',\omega'',s\rangle_3 \times[|\mathbf{q}+\mathbf{q}',\omega+\omega',0_X\rangle_4 + (-1)^{s+1}|\mathbf{q}+\mathbf{q}',\omega+\omega',1_X\rangle_4],$$

$$|\eta\rangle = \frac{Ng_2}{\sqrt{2}}\sum_s \int\int\int d\mathbf{q}d\mathbf{q}'d\mathbf{q}''\int\int\int d\omega d\omega' d\omega'' \times u(\mathbf{q},\omega,s)\Phi(\mathbf{q}',\omega',s^{\perp},\mathbf{q}'',\omega'',s^{\perp})|\mathbf{q}'',\omega'',s^{\perp}\rangle_3 \times[|\mathbf{q}+\mathbf{q}',\omega+\omega',0_X\rangle_5 + (-1)^{s}|\mathbf{q}+\mathbf{q}',\omega+\omega',1_X\rangle_5]. \tag{A5}$$

It is clear from these expressions that a measurement of the transverse wave vector, polarization, and frequency observables of photons 4 and 5 projects photon 3 in a state which is correlated with these measurement results. For instance, if we perform a destructive measurement which corresponds to the application of the annihilation operator $\mathbf{a}_{11}(\mathbf{q}_0,\omega_0) = \mathbf{a}_5(\mathbf{q}_0,\omega_0,1_X)$ on the state given by Eq. (A1), we find

$$|\psi_{11}\rangle \propto \mathbf{a}_{11}(\mathbf{q}_0,\omega_0)|\psi^{(1)}\rangle \propto \sum_s \int\int d\mathbf{q}d\mathbf{q}'\int\int d\omega d\omega' \times(-1)^s u(\mathbf{q},\omega,s)\Phi(\mathbf{q}_0-\mathbf{q},\omega_0-\omega,s^{\perp},\mathbf{q}',\omega',s^{\perp}) \times|\mathbf{q}',\omega',s^{\perp}\rangle_3. \tag{A6}$$

Next, Bob applies in photon 3 the unitary operation $\mathbf{U}_{11}(q_B,\omega_B)$ defined as

$$\mathbf{U}_{11}(\mathbf{q}_B,\omega_B)|\mathbf{q},\omega,s\rangle = \boldsymbol{\sigma}_Z\boldsymbol{\sigma}_X|\mathbf{q}+\mathbf{q}_B,\omega+\omega_B,s\rangle, \tag{A7}$$

which gives

$$|\psi_F^{11}\rangle \propto \mathbf{U}_{11}(q_B,\omega_B)|\psi_{11}\rangle \propto \sum_s \int\int d\mathbf{q}d\mathbf{q}'\int\int d\omega d\omega' u(\mathbf{q},\omega,s) \times\Phi(\mathbf{q}_0-\mathbf{q},\omega_0-\omega,s^{\perp},\mathbf{q}'-\mathbf{q}_B,\omega'-\omega_B,s^{\perp}) \times|\mathbf{q}',\omega',s\rangle_3, \tag{A8}$$

where we have used

$$\boldsymbol{\sigma}_Z\boldsymbol{\sigma}_X(-1)^s|\mathbf{q}',\omega',s^{\perp}\rangle_3 = (-1)^s|\mathbf{q}',\omega',(\boldsymbol{\sigma}_Z\boldsymbol{\sigma}_X)(s^{\perp})\rangle_3 = (-1)^s|\mathbf{q}',\omega',(\boldsymbol{\sigma}_Z)(s)\rangle_3 = |\mathbf{q}',\omega',s\rangle_3.$$

If, for instance,

$$\Phi(\mathbf{q},\omega,s,\mathbf{q}',\omega',s) = \frac{1}{\sqrt{2}}F(\mathbf{q},\mathbf{q}')G(\omega,\omega'), \tag{A9}$$

where

$$F(\mathbf{q},\mathbf{q}') \propto \delta^2(\mathbf{q}+\mathbf{q}'-\mathbf{q}_p),$$

$$G(\omega,\omega') \propto \delta(\omega+\omega'-\omega_p). \tag{A10}$$

we then find

$$|\psi_F^{11}\rangle \propto \sum_s \int d\mathbf{q}\int d\omega u(\Delta\mathbf{q}-\mathbf{q}_B,\Delta\omega-\omega_B,s)|\mathbf{q},\omega,s\rangle_3, \tag{A11}$$

where $\Delta\mathbf{q}\equiv\mathbf{q}+\mathbf{q}_0-\mathbf{q}_p$ and $\Delta\omega\equiv\omega+\omega_0-\omega_p$. Using the shifts $\mathbf{q}_B=\mathbf{q}_0-\mathbf{q}_p$ and $\omega_B=\omega_0-\omega_p$, we finally obtain

$$|\psi_F^{11}\rangle \propto |\phi\rangle_3 \tag{A12}$$

which corresponds to a perfect teleportation.

2. SFG in type-I (II) crystals

Equation (36) describes in certain approximations the effective Hamiltonian governing the process of SFG in nonlinear crystals. If it is a type-I crystal, two photons with the same polarization are destroyed, and another one with an orthogonal polarization related to the destroyed one is created, the polarization orientation being given by the crystal axis. As result, if two crystals with orthogonal axis are combined, the Hamiltonian which describes SFG will be

$$\mathbf{H} = A \sum_{s=H,V} \int\int d\mathbf{q}d\mathbf{q}' \int\int d\omega d\omega' \mathbf{a}_1(\mathbf{q},\omega,s)\mathbf{a}_2(\mathbf{q}',\omega',s) \times \mathbf{a}_4^{\dagger}(\mathbf{q}+\mathbf{q}',\omega+\omega',s^{\perp}) + \text{H.c.}, \tag{A13}$$

which is precisely the form of Eq. (9). An equivalent argument shows that Eq. (10) is obtained when two type-II nonlinear crystals cut for SFG are combined.

[1] C. H. Bennett, G. Brassard, C. Crépeau, R. Jozsa, A. Peres, and W. K. Wootters, Phys. Rev. Lett. **70**, 1895 (1993).
[2] D. Gottesman and I. L. Chuang, Nature (London) **402**, 390 (1999).
[3] E. Knill, R. Laflamme, and G. J. Milburn, Nature (London) **409**, 46 (2001).
[4] N. Yoran and B. Reznik, Phys. Rev. Lett. **91**, 037903 (2003).
[5] H. J. Briegel, W. Dür, J. I. Cirac, and P. Zoller, Phys. Rev. Lett. **81**, 5932 (1998).
[6] D. Bouwmeester, J. Pan, K. Mattle, M. Eibl, H. Weinfurter, and A. Zeilinger, Nature (London) **390**, 575 (1997).
[7] D. Boschi, S. Branca, F. DeMartini, L. Hardy, and S. Popescu, Phys. Rev. Lett. **80**, 1121 (1998).
[8] Y.-H. Kim, S. P. Kulik, and Y. Shih, Phys. Rev. Lett. **86**, 1370 (2001).
[9] I. Marcikic, H. de Riedmatten, W. Tittel, H. Zbinden, and N. Gisin, Nature (London) **421**, 509 (2003).
[10] R. Ursin, T. Jennewein, M. Aspelmeyer, R. Kaltenbaek, M. Lindenthal, P. Walther, and A. Zeilinger, Nature (London) **430**, 849 (2004).
[11] A. Furusawa, J. L. Sorensen, S. L. Braunstein, C. A. Fuchs, H. J. Kimble, and E. S. Polzik, Science **282**, 706 (1998).
[12] M. Yukawa, H. Benichi, and A. Furusawa, Phys. Rev. A **77**, 022314 (2008).
[13] P. G. Kwiat, J. Mod. Opt. **44**, 2173 (1997).
[14] J. T. Barreiro, N. K. Langford, N. A. Peters, and P. G. Kwiat, Phys. Rev. Lett. **95**, 260501 (2005).
[15] L. Lamata, J. J. García-Ripoll, and J. I. Cirac, Phys. Rev. Lett. **98**, 010502 (2007).
[16] S. P. Walborn, D. S. Ether, R. L. de Matos Filho, and N. Zagury, Phys. Rev. A **76**, 033801 (2007).
[17] I. V. Sokolov, M. I. Kolobov, A. Gatti, and L. A. Lugiato, Opt. Commun. **193**, 175 (2001).
[18] L. V. Magdenko, I. V. Sokolov, and M. I. Kolobov, Opt. Spectrosc. **103**, 62 (2007).
[19] B. E. A. Saleh and M. C. Teich, *Fundamental of Photonics* (Wiley, Interscience, Hoboken, NJ, 2007).
[20] A. Einstein, D. Podolsky, and N. Rosen, Phys. Rev. **47**, 777 (1935).
[21] L. Davidovich, N. Zagury, J. M. Raimond, and S. Haroche, Phys. Rev. A **50**, R895 (1994).
[22] P. G. Kwiat, K. Mattle, H. Weinfurter, A. Zeilinger, A. V. Sergienko, and Y. Shih, Phys. Rev. Lett. **75**, 4337 (1995).
[23] P. G. Kwiat, E. Waks, A. G. White, I. Appelbaum, and P. H. Eberhard, Phys. Rev. A **60**, R773 (1999).
[24] R. W. Boyd, *Nonlinear Optics* (Academic, New York, 1992).
[25] C. H. Monken, P. H. Souto Ribeiro, and S. Pádua, Phys. Rev. A **57**, 3123 (1998).
[26] C. K. Hong and L. Mandel, Phys. Rev. A **31**, 2409 (1985).
[27] Z. Y. Ou, L. J. Wang, and L. Mandel, Phys. Rev. A **40**, 1428 (1989).
[28] L. J. Wang, X. Y. Zou, and L. Mandel, Phys. Rev. A **44**, 4614 (1991).
[29] D. S. Ether, P. H. Souto Ribeiro, C. H. Monken, and R. L. de Matos Filho, Phys. Rev. A **73**, 053819 (2006).
[30] Z. Y. Ou, Phys. Rev. A **78**, 023819 (2008).
[31] H. Dong, H. Pan, H. Z. Y. Li, and E. Wu, Appl. Phys. Lett. **93**, 071101 (2008).
[32] M. C. de Oliveira, Phys. Rev. A **67**, 022307 (2003).
[33] L. Deng, E. W. Hagley, J. Wen, M. Trippenbach, Y. Band, P. S. Julienne, J. E. Simsarian, K. Helmerson, S. L. Rolston, and W. D. Phillips, Nature (London) **398**, 218 (1999).
[34] Y. Castin and J. Dalibard, Phys. Rev. A **55**, 4330 (1997).
[35] T. S. Humble, R. S. Bennink, W. P. Grice, *Proceedings of SPIE, The International Society of Optical Engineering*, (2008) Vol. 7092.